



ELSEVIER

Available online at [www.sciencedirect.com](http://www.sciencedirect.com)

SCIENCE @ DIRECT®

Nuclear Instruments and Methods in Physics Research B 210 (2003) 336–342

**NIM B**  
Beam Interactions  
with Materials & Atoms

[www.elsevier.com/locate/nimb](http://www.elsevier.com/locate/nimb)

## Trace elemental distributions in induced atherosclerotic lesions using nuclear microscopy <sup>☆</sup>

Ren Minqin <sup>a</sup>, Frank Watt <sup>a,\*</sup>, Benny Tan Kwong Huat <sup>b</sup>, B Halliwell <sup>c</sup>

<sup>a</sup> Department of Physics, Research Centre for Nuclear Microscopy, National University of Singapore, Lower Kent Ridge Road, Singapore 119260, Singapore

<sup>b</sup> Department of Pharmacology, National University of Singapore, Singapore, Singapore

<sup>c</sup> Department of Biochemistry, National University of Singapore, Singapore, Singapore

### Abstract

Nuclear Microscopy, using the combination of scanning transmission ion microscopy, Rutherford backscattering spectrometry and proton induced X-ray emission has the ability to map and accurately quantify localised trace element levels in newly formed atherosclerotic lesions. In this study, New Zealand white rabbits fed on a high cholesterol diet were divided into two groups. One test group was treated with an iron chelating agent *desferal*, and the second group served as a control model. Tissue sections were taken from the aortic arch, flash frozen and air-dried, and scanned using the nuclear microscope of the Research Centre for Nuclear Microscopy, NUS. Results of this experiment, although not definitive ( $p = 0.07$ ) indicated that during the treatment with *desferal*, there was a trend for lesion development to be slowed down. However, analysis of atherosclerotic lesions both from the test and control groups showed that iron concentrations within the lesions exhibit a high degree of correlation with the depth of the lesion in the artery wall, whereas zinc is observed to be anti-correlated to the size of the lesion area. This investigation implies that the observed high iron levels, which can lead to increased free radical damage, may cause premature or accelerated arterial damage. © 2003 Elsevier B.V. All rights reserved.

**Keywords:** Trace element distributions; Nuclear Microscopy; Atherosclerosis; Iron; Iron chelation; Desferal

### 1. Introduction

There is an increasing body of evidence that indicates that iron may play an important role in atherosclerosis through the catalysis of cytotoxic free radicals [1–7]. Unregulated ferric iron has the

ability to promote the oxidation of low-density lipoprotein [8,9] resulting in the formation of atherosclerotic plaques leading to arterial degeneration. Although several epidemiological studies have suggested that elevated tissue iron levels may increase the risk for atherosclerosis [10–12], there are some contrasting studies which indicate otherwise [13,14]. The hypothesis is therefore controversial.

This paper describes on-going work carried out at Research Centre for Nuclear Microscopy, National University of Singapore, into the trace elemental distributions in induced atherosclerotic

<sup>☆</sup> Presented at the 8th International Conference on Nuclear Microprobe Technology and Applications, Takasaki, Japan September 2002.

\* Corresponding author. Tel.: +65-6874-2815; fax: +65-6777-6126.

E-mail address: [phywattf@nus.edu.sg](mailto:phywattf@nus.edu.sg) (F. Watt).

lesions using the elemental analysis capability of nuclear microscopy. Previous work by us has shown that early atherosclerotic lesions, induced by feeding New Zealand White rabbits on a 1% cholesterol diet, contain increased levels of iron (up to eight times) compared with the adjacent healthy artery wall [15,16]. In a follow-up time sequence study, we have shown that iron accumulation occurs at the onset of lesion formation, which takes place around 4–6 weeks after exposure to the 1% cholesterol diet. As the lesions mature, they enlarge to occupy a significant fraction of the artery wall, and at about 16 weeks the lesions begin to show signs of calcification. In an additional experiment, where the cholesterol fed rabbits were kept anaemic through weekly bleeding, the iron content of the artery wall was reduced and the onset of atherogenesis was delayed [1].

Experimental work from other groups suggests that the iron chelator *desferal* can protect against tissue injury [17–20], since *desferal* forms a stable complex with ferric iron, decreasing its availability for the production of reactive free radicals [21]. We have therefore used *desferal* in a further investigation, where rabbits were fed on a 1% cholesterol diet and after 6 weeks (corresponding to the period of early lesion formation) a test group was subjected to chelation treatment. This use of *desferal* to treat induced atherosclerosis in rabbits showed that there was a trend for lesion development to be slowed down, although these results were not definitive ( $p = 0.07$ ) [22]. During the course of this study we observed that the atherosclerotic lesions did not develop at a consistent rate for animals in the same group, and further that the lesions were not of a consistent size when measured at different parts of the same artery. We did observe however a consistent and significant relationship between the size of the developed lesions and the localized trace element content of zinc and iron in the lesions. The methodology and results of this work are presented here.

## 2. Experiment and method

Sixteen New Zealand White rabbits weighing on average 2.5 kg, were fed a diet of 1% high

cholesterol food. Six weeks into the diet, the rabbits were each surgically implanted with Alzet osmotic pumps (Qisa Corporation, Palo Alto USA) containing the iron chelator *desferal* (0.5 g/ml) for the test group (eight rabbits), and saline for the control group (eight rabbits). *Desferrioxamine* (as *desferal*<sup>®</sup>, *desferrioxamine B methanesulphonate*) was obtained from Novartis Pharma Ag Basle, Switzerland. Four test group rabbits and four control group rabbits were sacrificed 2 weeks after the pump implantation. These groups were named the 8-week control group and the 8-week test group. Three test group rabbits and three control group rabbits were sacrificed 4 weeks after pump implantation (one rabbit from each group did not survive the 10-week term). These groups were named the 10-week test group and 10-week control group. Animals were sacrificed by *i/v* injection of sodium pentobarbitone (0.8 mg/kg). The aortic arch was removed and cut into three segments (A, B and C). Segments were quickly flushed with de-ionized water to remove residual blood from the inner artery wall, and flash frozen in liquid nitrogen. This animal study was approved by the local animal care and use committee of the National University of Singapore.

Ten micron sections from the flash frozen tissue blocks were cut by cryo-sectioning, mounted on nuclear microscope holders, and air dried prior to the nuclear microscopy scans. The nuclear microscopy investigations were carried out using a 2 MeV proton beam focused to a 1- $\mu\text{m}$  spot size, and utilized three complementary ion beam techniques which were simultaneously applied: (a) Off-axis scanning transmission ion microscopy (STIM) provided information on the structure and density distribution of the sample and facilitated positioning of the unstained sections prior to analysis. The STIM maps were also used for lesion size determinations (see below). (b) Particle induced X-ray emission (PIXE) was used for measuring the concentrations of elements, and in particular the trace elements Fe and Zn. The tissue section was positioned at 45° with respect to the beam axis to maximize the X-ray detection efficiency, and a 300  $\mu\text{m}$  Perspex filter with a 1-mm-diameter central hole was used with the 61 mm<sup>2</sup> Si(Li) X-ray detector to optimize the system for the detection of

trace elements from Ca to Zn [23]. (c) Rutherford backscattering spectrometry (RBS) provided information on matrix composition and incident charge and was used to extract quantitative results in conjunction with PIXE.

### 3. Results

Previous results have shown that the measured lesion size not only varied from animal to animal but also varied inside the aortic arch of the same animal [22]. The average lesion area for the 8-week control group was  $2.0 \pm 0.5 \text{ mm}^2$  increasing to a value of  $5.4 \pm 1.1 \text{ mm}^2$  for the 10-week control group. The average lesion area for the 8 week test group was  $2.7 \pm 0.5 \text{ mm}^2$  rising to  $3.55 \pm 0.6 \text{ mm}^2$  for the 10-week test group [22]. A two sample student-*t* test yielded a difference in the 10 week controls compared with the 10 week test samples

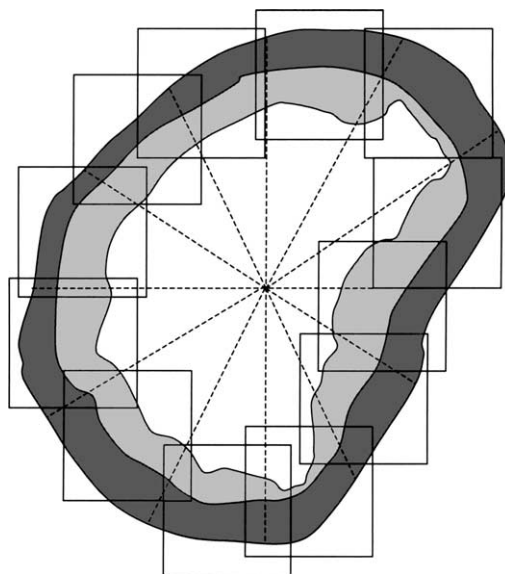


Fig. 1. Schematic diagram showing the use of multiple scans to extract elemental data from the lesion and adjacent artery wall.

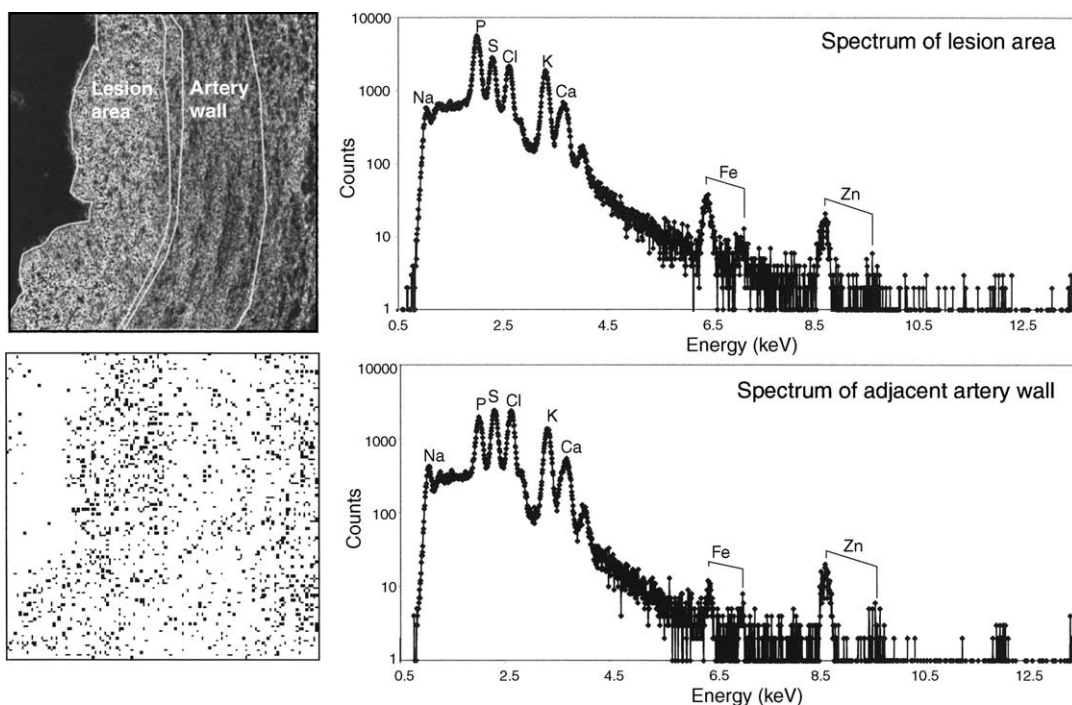


Fig. 2. Top left: example of STIM map of scanned area of aortic arch section showing the masks used to extract data from the lesion and the artery wall, bottom left: iron map of the same area, top right and bottom right: PIXE spectra of the lesion and the artery wall extracted from the masked areas.

in the  $0.05 < p_t < 0.1$  range ( $p = 0.07$ ). While this did not represent a definitive result, it suggested a trend for the rabbits undergoing 4 weeks desferal therapy to exhibit a decrease in the rate of lesion development.

Further analysis was undertaken on the 10-week group animals, for both test (1% cholesterol fed with desferal treatment after 6 weeks) and control (1% cholesterol fed with no desferal treatment). One aortic arch section from each of the six animals in this group was studied in more detail. Since we required detailed elemental distributions, scan sizes were kept to less than our maximum scan size of  $4 \text{ mm} \times 4 \text{ mm}$ . We therefore scanned the whole inner wall lesion on an area by area basis, accumulating the data utilizing list mode data handling techniques [24]. From this data we were able to extract quantitative elemental data from up to 16 areas around the lesion (schematically shown in Fig. 1). An example of the off-line data extraction process is depicted in Fig. 2, which shows typical masked areas for the lesion and the artery wall (top left), with the iron map of

the scanned area (bottom left) and PIXE spectra extracted from the lesion and the adjacent artery wall (right top and bottom). From each of the scanned areas we also extracted the average depth of lesion from the STIM maps, the lesion depths calculated from an average of 10 depth measurements per area. A graph of the iron concentrations plotted against average depth of the lesion for each scanned area (shown in Fig. 3) shows a positive correlation for all six animals. A graph of zinc concentrations plotted against lesion depth for each area studied is shown in Fig. 4, and shows a negative correlation for five out of the six animals. *Pearson correlation* analysis of all the data shows a strong and significant correlation between iron levels and the depth of lesion and anti-correlation between zinc and lesion depth.

As an indication of the elemental concentrations obtained from these data, Table 1 shows the elemental concentrations extracted from those scanned areas that exhibited the smallest depth of lesion (least lesion development), and Table 2 shows the elemental concentrations extracted from

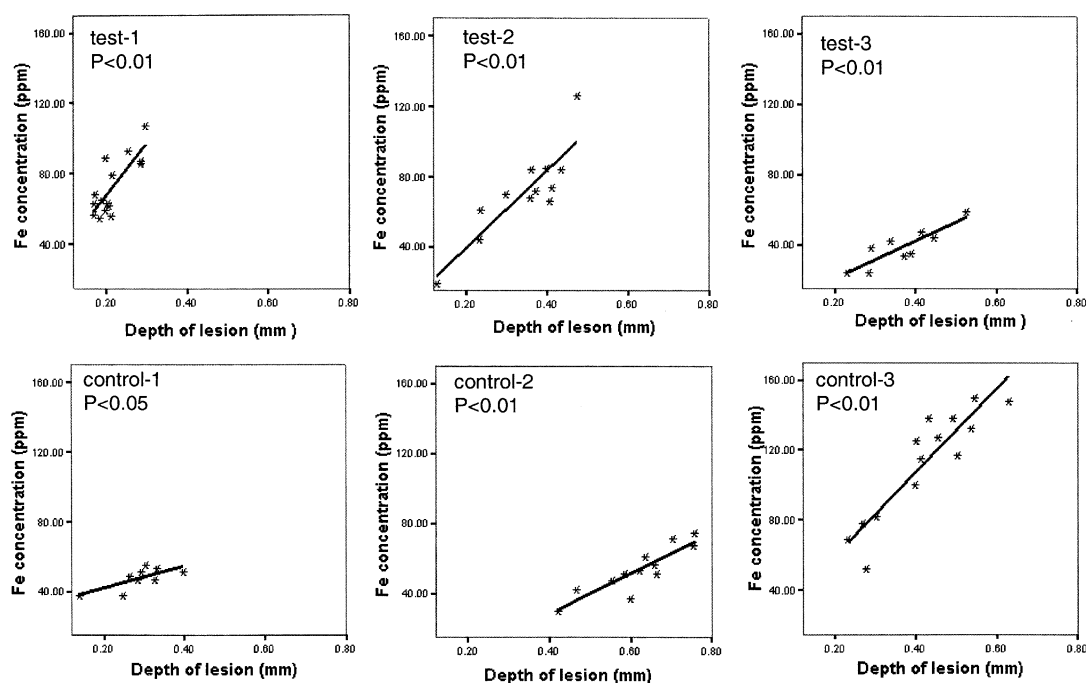


Fig. 3. Pearson correlation between Fe concentration (parts per million, dry weight) and the depth of the lesion.

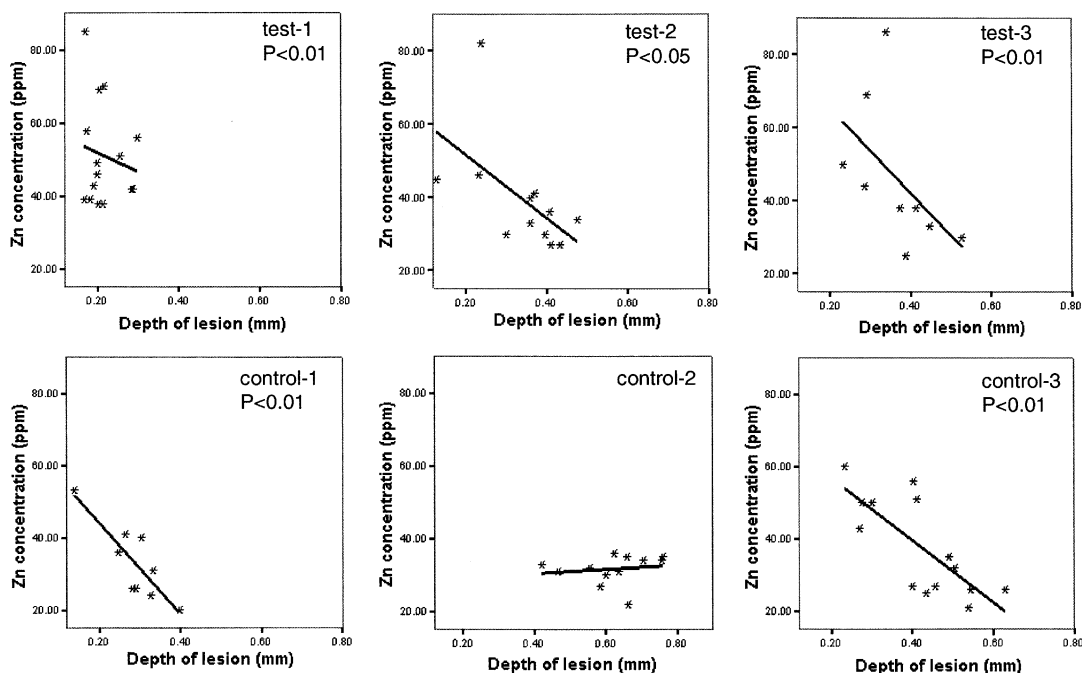


Fig. 4. Pearson correlation between Zn concentration (parts per million, dry weight) and the depth of the lesion.

Table 1

Elemental concentrations (lesion and artery wall) taken from the region of aortic arch that exhibited the least developed lesion

	Test-1		Test-2		Test-3	
	Lesion	Artery	Lesion	Artery	Lesion	Artery
<i>Test models</i>						
P	12,461 (37)	6926 (37)	7210 (57)	5365 (42)	5204 (42)	2930 (30)
S	5948 (32)	11,762 (47)	4641 (51)	8308 (50)	4293 (40)	6158 (39)
Cl	6425 (32)	12,566 (50)	4876 (54)	10,057 (57)	3210 (38)	5057 (38)
K	2249 (15)	3805 (22)	4352 (39)	7119 (36)	1959 (20)	2108 (17)
Ca	807 (11)	1110 (15)	468 (21)	637 (22)	374 (11)	444 (10)
Fe	57 (3)	18 (2)	19 (4)	15 (3)	24 (3)	2 (2)
Cu	<6	5 (2)	<7	8 (3)	<5	6 (2)
Zn	40 (4)	189 (8)	46 (8)	153 (9)	50 (5)	94 (5)
	Control-1		Control-2		Control-3	
	Lesion	Artery	Lesion	Artery	Lesion	Artery
<i>Control models</i>						
P	6862 (46)	3890 (35)	9830 (69)	7108 (105)	7425 (70)	5120 (52)
S	5014 (43)	7092 (43)	5187 (58)	10,507 (128)	7170 (72)	9463 (65)
Cl	2473 (36)	4651 (40)	4737 (55)	11,692 (138)	6243 (72)	8444 (66)
K	1381 (20)	1403 (18)	2182 (24)	3778 (51)	3483 (39)	4668 (36)
Ca	460 (14)	625 (13)	298 (12)	534 (26)	760 (23)	733 (20)
Fe	39 (3)	17 (2)	32 (3)	25 (5)	53 (6)	13 (3)
Cu	<6	7 (3)	<4	<10	<9	8 (4)
Zn	54 (6)	112 (8)	27 (4)	85 (13)	51 (10)	114 (9)

Concentrations are in part per million dry weight and errors are in brackets.

Table 2

Elemental concentrations (lesion and artery wall) taken from the region of aortic arch that exhibited the most developed lesion

	Test-1		Test-2		Test-3	
	Lesion	Artery	Lesion	Artery	Lesion	Artery
<i>Test group (three rabbits)</i>						
P	14,004 (34)	8113 (60)	8568 (26)	5177 (64)	6617 (23)	5172 (39)
S	6467 (29)	11,929 (73)	3515 (20)	7902 (77)	4283 (21)	8660 (48)
Cl	6556 (28)	11,000 (77)	3792 (20)	10,264 (90)	3259 (19)	7526 (48)
K	3073 (14)	4148 (37)	2735 (13)	5406 (51)	2191 (10)	3824 (23)
Ca	1400 (12)	1145 (24)	2403 (13)	1015 (30)	321 (7)	655 (14)
Fe	107 (3)	28 (4)	74 (2)	25 (6)	60 (2)	12 (2)
Cu	10 (2)	13 (5)	<2	<13	2 (1)	4 (3)
Zn	56 (4)	188 (13)	27 (2)	69 (11)	30 (2)	100 (6)
<i>Control group (three rabbits)</i>						
	Control-1		Control-2		Control-3	
	Lesion	Artery	Lesion	Artery	Lesion	Artery
P	6585 (25)	4569 (50)	14,599 (61)	8889 (125)	11,198 (44)	6984 (79)
S	3642 (22)	7419 (61)	6880 (48)	15,506 (160)	5695 (36)	9761 (92)
Cl	1917 (19)	5565 (60)	7054 (47)	17,168 (172)	5961 (38)	10,767 (102)
K	1099 (10)	1788 (28)	2885 (20)	4750 (59)	3157 (20)	4862 (51)
Ca	585 (8)	583 (18)	8630 (28)	1119 (33)	1085 (14)	622 (27)
Fe	51 (2)	30 (4)	68 (3)	59 (7)	149 (4)	95 (8)
Cu	<2	<10	16 (3)	<12	<3	14 (7)
Zn	21 (2)	78 (10)	34 (4)	94 (15)	27 (4)	121 (13)

Concentrations are in part per million dry weight and errors are in brackets.

the scans over the areas that exhibited the largest depth of lesion (maximum lesion development). From these results we can see that the average Fe concentration of the most developed lesions is 85 ppm, whereas the average Fe concentrations of the least developed lesions is 37 ppm. From these tables we also observe that in all cases the lesion contains a higher concentration of iron than the adjacent artery wall, whereas the lesion contains less zinc than the artery wall.

#### 4. Discussion

Analysis of atherosclerotic lesions induced in New Zealand White rabbits shows that iron concentrations within the developing lesion are observed to have a high degree of correlation with the depth of the lesion in the artery wall. This observed correlation implies that the observed increased levels of iron could lead to increased free radical damage, thereby causing premature or accelerated arterial damage. Iron therefore, as a

catalyst in the formation of free radicals that subsequently modify LDL cholesterol, could play a significant role in atherogenesis, since enhanced iron-mediated oxidative stress and LDL peroxidation may contribute to hypercholesterolemia-related endothelial dysfunction. Interestingly, the observed anti-correlation of the observed depth of the lesion with zinc is consistent with other work suggesting that zinc has a possible anti-atherosclerotic effect [25,26].

#### References

- [1] D. Ponraj, J. Makjanic, P.S.P. Thong, B.K.H. Tan, F. Watt, *FEBS Lett.* 459 (1999) 218.
- [2] M. Roest, Y.T. van der Schouw, B. de Valk, J.J.M. Marx, M.J. Templeman, P.G. de Groot, J.J. Sixma, J.D. Banga, *Circulation* 100 (1999) 1268.
- [3] T.P. Tuomainen, K. Kontula, K. Nyyssonen, T.A. Lakka, T. Helio, J.T. Salonen, *Circulation* 100 (1999) 1274.
- [4] J.W. Heinecke, H. Rosen, A. Chait, *J. Clin. Invest.* 74 (1984) 1890.
- [5] B.J. Van Lenten et al., *J. Clin. Invest.* 95 (1995) 2104.

- [6] J.W. Heniecke, L. Baker, H. Rosen, A. Chait, *J. Clin. Invest.* 77 (1986) 757.
- [7] T.S. Lee, M.S. Shiao, C.C. Pan, et al., *Circulation* 99 (1999) 1222.
- [8] B. Halliwell, J.M. Gutteridge, *Biochem. J.* 219 (1) (1984) 1.
- [9] B. Halliwell, J.M. Gutteridge, *Free Radicals in Biology and Medicine*, 3rd ed., Oxford University, 1999, Chapters 2 and 3.
- [10] J.L. Sullivan, *Am. Heart J.* 117 (1989) 1177.
- [11] P. Ponka, C. Beaumont, D.R. Richardson, *Semin. Hematol.* 35 (1998) 35.
- [12] J.T. Salonen, H. Korpela, K. Nyysönen, et al., *J. Intern. Med.* 237 (1995) 161.
- [13] E. Rossi, B.M. McQuillan, J. Hung, P.L. Thompson, C. Kuek, J.P. Beilby, *Stroke* 31 (2000) 3015.
- [14] J. Danesh, P. Appleby, *Circulation* 99 (1999) 852.
- [15] F. Watt, M. Selley, P.S.P. Thong, S.M. Tang, *Nucl. Instr. and Meth. B* 104 (1995) 356.
- [16] P.S.P. Thong, M. Selley, F. Watt, *Cell. Mol. Biol.* 42 (1996) 103.
- [17] B. Halliwell, *Free Radic. Biol. Med.* 7 (6) (1989) 645.
- [18] L.D. Horwitz, E.A. Rosenthal, *Vasc. Med.* 4 (1999) 93.
- [19] J.L. Sullivan, *Am. Heart J.* 143 (2) (2002) 193.
- [20] S. Sanan, G. Sharma, R. Malhotra, D.P. Sanan, P. Jain, P. Vadhera, *Free Radic. Res. Commun.* 6 (1) (1989) 29.
- [21] B. Halliwell, *Biochem. Pharmacol.* 34 (1985) 229.
- [22] F. Watt, M.Q. Ren, J.P. Xie, B.K.H. Tan, B. Halliwell, *Nucl. Instr. and Meth. B* 181 (2001) 431.
- [23] F. Watt, *Nucl. Instr. and Meth. B* 104 (1995) 276.
- [24] G.W. Grime, M. Dawson, *Nucl. Instr. and Meth. B* 89 (1994) 223.
- [25] B. Hennig, M. Toborek, C.J. McClain, *Nutrition* 12 (10) (1996) 711.
- [26] T.M. Bray, W.J. Bettger, *Free Radic. Biol. Med.* 8 (3) (1990) 281.